

## Generator Excitation Control Method based on Iterative Learning Control with Initial State Learning and Model-free Adaptive Grey Prediction Control

Jingcai Bai\*, Junxiao Wu, Guozhu Wang and Yongtao Hu

Department of Automatic Control, Henan Institute of Technology, Xinxiang 453003, China

Received 12 July 2018; Accepted 29 September 2018

### Abstract

In a synchronous generator excitation control system, the damping capacity of the system is generally weakened during high-accuracy regulation of terminal voltage, which is against system stability. In this study, an excitation control method based on iterative learning control (ILC) with initial state learning and model-free adaptive grey prediction control (MFAGPC) was proposed to achieve high-accuracy voltage regulation and system stability. Based on the third-order dynamic model of generators, an excitation control system was constructed. The system used ILC as primary controller and MFAGPC as secondary controller to design the terminal voltage and rotor speed, respectively. Furthermore, the influences of ILC and MFAGPC on the regulation accuracy of terminal voltage and system stability were discussed. The proposed control method was validated by simulation and experimentation. The results demonstrate that under the conventional PID+PSS, the overshoot and settling time of the terminal voltage are 32% and 2.6s, and the rotor speed undergoes 6 oscillations in 4.3s before the system returns to a stable state. Due to the synergic effect of ILC and MFAGPC, the overshoot and settling time of the terminal voltage are 7% and 0.7s, and the rotor speed just undergoes 3 oscillations in 2.5s before the system returns to steady state. The proposed control method assures that the system achieves adequate regulation accuracy of terminal voltage in a short time, overcomes influences of internal and external disturbances on the system, and enhances system stability. This study provides a reference for further studies on multi-goal control problems of power systems.

*Keywords:* Excitation control, Iterative learning control, Model-free adaptive control, Grey prediction, GM (2,1) model

### 1. Introduction

Synchronous generator excitation control has attracted attention in the academe in the past 50 years. The tasks of excitation control have shifted from simple maintenance of the terminal voltage in the past to high-accuracy voltage regulation at present considering oscillation inhibition and improvement of system stability. Maintaining the terminal voltage and enhancing the stability of power system are tasks that have to be performed consistently. However, the damping torque is inadequate to deteriorate the system stability when the terminal voltage keeps constant [1]. At present, adding excitation control in the excitation control system is an effective measure. PID+PSS control [2] and linear optimal excitation control [1] are representative methods that have approximate linearization of the power system close to the equilibrium point. When the power system is disturbed from its original state point, these linear models may generate large deviations and a significant reduction in the control effect.

Thus, nonlinear excitation control theory has been studied extensively in the last two decades. The excitation controller is designed by differential geometry method in nonlinear excitation control in reference [3]. In the past, direct feedback linear method [4], Hamilton system theory [5], variable structure control [6] and backstepping method

[7-8] were applied in nonlinear excitation control successively. However, these nonlinear excitation control methods return the power angle of a recovering generator to the original angle before disturbance. System parameters and control method may change upon disturbance. Although the system can realize the finite stabilization of disturbance, this may cause the terminal voltage to deflect from the desired value. The principal tasks of the generator excitation system are to enhance system stability and satisfy the regulation accuracy of terminal voltage. These two tasks are often contradictory. The goal of the control focuses either on the power angle or on the terminal voltage to improve the stability of power system or satisfy the regulation accuracy of voltage, which has disadvantages. Voltage should be designed as an independent and master control to ensure the regulation accuracy.

Thus, a new excitation control method is proposed by studying the multi-objective control problem. This method takes the terminal voltage as the master control variable that can enhance the system stability during high-accuracy regulation of voltage.

### 2. State of the art

Plenty of experts have discussed the stability of power system and the regulation accuracy of terminal voltage. Mahmud [9] designed an excitation controller based on the partial feedback linearization method and obtained good excitation stabilization by combining the observer, but the

\*E-mail address: okbjrc@163.com

ISSN: 1791-2377 © 2018 Eastern Macedonia and Thrace Institute of Technology. All rights reserved.

doi:10.25103/jestr.114.04

uncertainties existing in the power system model were ignored. Considered the uncertainties within system, Su [10] demonstrated the finite stabilization of the fault by using the high-order sliding mode but failed to achieve ideal stabilizing terminal voltage. Zhao [11] combined the sliding mode variable structure and AVR into the excitation system of a waste heat generator unit. The method could track the given signal well but did not eliminate the adverse effects of buffeting. Alden [12] studied the power system with feedback delay and proposed a robust control based on linear matrix inequality, which achieved transient stability effectively. However, obtaining the boundary information of the uncertain parts in the actual control system was difficult, thereby resulting in conservation of the robust controller design. Peng [8] designed the excitation controller by random nonlinear integral backstepping method. This controller could partially inhibit random disturbance in the system. Masrob[13] and Zhao[14] developed an artificial neural network power system stabilizer (PSS) and a predictive excitation controller to improve system stability by reducing order in the power system model. However, the regulation of terminal voltage was not viewed as a master control. Ghasemi [15] and Kumar [2] optimized the PSS parameters by fuzzy gravity search algorithm and local information of each machine in a multi-machine environment, and solved the combination optimization problem. However, the input constraints of the system were neglected. Zhao [16] introduced the model-free adaptive control (MFAC) into the design of wide-area PSS, which inhibited the inter-area low-frequency oscillation effectively. However, the influence of the wide-area PSS on terminal voltage was not analyzed. Guo [17] applied the nonlinear excitation controller based on the deviation separation for power system considering model deviation and disturbance deviation. The controller could inhibit disturbance of the power system to a certain extent, but the deduction process of control law was complicated and the power angle was difficult to measure. Zhang [18] applied an improved MFAC algorithm into the marine generator excitation system, which had certain fault tolerance to data distortion and load change. However, the voltage regulation was absent. Wang [19] introduced the differential evolution mechanism to optimize the automatic voltage regulation system by PID. Lin [20] combined the Adams prediction model and MFAC with the generator excitation control system. The aforementioned two methods improved the regulation accuracy of terminal voltage but ignored the multi-objective requirements of the power system. Based on the differential geometry and expansion state observer, Chang [21] designed a dummy controlled variable using variable structure theory, and added the deviation control of the terminal voltage to ensure transient stability and voltage regulation. However, the effect in stabilizing terminal voltage failed, and the process involved multiple parameters and complex operations. To avoid measurement of the power angle, Ruan [22] and Yang [23] designed the excitation controller by nonlinear output feedback method to ensure the transient stability and the regulation accuracy of terminal voltage. However, uncertainty features were neglected in the operation.

The results mentioned were based on the control goal of the terminal voltage or the power angle. Such an excitation system design based on a single control goal cannot satisfy the performance of the power system. Moreover, the proposed algorithms were extremely complicated and had numerous parameters. Recently, iterative learning control (ILC) and MFAC have attracted the attention of many

scholars. Independent of an accurate mathematical model of the controlled system, ILC can search the ideal control signal through a learning law and a repeated training process based on previous control experiences and the measured tracking error signal. Therefore, the controlled system could output a high-accuracy track in limited time with a simple and easy algorithm [24]. MFAC does not need to construct the precise mathematical model of nonlinear system and could realize an adaptive control of complicated nonlinear system by using the input and output data in the operating process. As MFAC is unrelated to any state in the process, it is free from external disturbances and is robust. A few parameters in the algorithm could be easily fine-tuned [18, 25]. Considering conditions such as nonlinearity, time variation, and difficulty of establishing a precise model, ILC and MFAC were combined and applied to the generator excitation control system based on complete analysis of the tasks and characteristics of the excitation system. The excitation controller had a primary and a secondary control loop. The primary control loop used high-accuracy tracking of terminal voltage by ILC, while the secondary control loop transformed the system into a robust structure not influenced by internal and external disturbances of the MFAC of rotor speed. With the advantages of grey prediction, a GM(2,1) model is added in the feedback loop of the MFAC, thus forming model-free adaptive grey prediction control (MFAGPC). The GM(2,1) model is used to predict and compensate the system in the presence of time varying of parameters, system delays, and overshooting to improve the system performance.

The remainder of this study is organized as follows. Section 3 establishes the third-order nonlinear model of synchronous generator and analyzes the ILC design of terminal voltage as well as the MFAGPC design of rotor speed. Section 4 introduces the simulation and experimentation of the proposed control method. Conclusions are summarized in Section 5.

### 3. Methodology

#### 3.1 Power system model

When the equivalent damping winding  $g$ ,  $D$ , and  $Q$  are disregarded, only winding  $f$  and the dynamic equation of rotor are considered, and the input mechanical power are assumed constant, the third-order dynamic model of the  $i$ th generator [26] can be written as

$$\begin{cases} \dot{\delta}_i = \omega_i - \omega_0 \\ \dot{\omega}_i = \frac{\omega_0}{H_i}(P_{mi} - P_{ei}) - \frac{D_i}{H_i}(\omega_i - \omega_0) \\ \dot{E}'_{qi} = \frac{1}{T'_{d0i}} \left[ U_{fi} - E'_{qi} - \frac{(x'_{di} - x'_{d\sigma})}{x'_{d\sigma}} U_s \cos \delta_i \right] \end{cases} \quad (1)$$

The relevant algebraic equations during the steady-state conditions can be written as

$$i'_{di} = \frac{E'_{qi} - U_s \cos \delta_i}{x'_{d\sigma}}$$

$$\begin{aligned}
 i_{qi} &= \frac{U_s \sin \delta_i}{x_{q\Sigma}} \\
 U_{di} &= x_{qi} i_{qi} \\
 U_{qi} &= E'_{qi} - x'_{di} i_{di} \\
 U_{ii}^2 &= U_{di}^2 + U_{qi}^2 \\
 P_{ei} &= U_{di} i_{di} + U_{qi} i_{qi} = \frac{E'_{qi}}{x'_{d\Sigma}} U_s \sin \delta_i
 \end{aligned} \tag{2}$$

where  $\delta_i$ ,  $\omega_i$ , and  $E'_{qi}$  are state variables, which denote the power angle, rotor speed of rotor, and  $q$ -axis transient potential of the  $i$ th generator, respectively.  $U_{fi}$  and  $U_{ii}$  are the excitation voltage and terminal voltage of the  $i$ th generator.  $U_s$  is the infinite bus voltage.  $P_{mi}$  is the mechanical input power of the  $i$ th generator, which is assumed to be constant.  $P_{ei}$  is the active power generated by the  $i$ th generator.  $H_i$  is the inertia constant of the  $i$ th generator.  $D_i$  is the damping coefficient of the  $i$ th generator.  $T'_{d0i}$  is the  $d$ -axis open-circuit transient time constant of the stator in the  $i$ th generator.  $x_{di}$  and  $x'_{di}$  are  $d$ -axis synchronous reactance and transient reactance of the  $i$ th generator.  $x_{qi}$  is the  $q$ -axis synchronous reactance of the  $i$ th generator.  $x_T$  and  $x_L$  are the total reactance of transformer and transmission line,  $x'_{d\Sigma} = x'_{di} + x_T + x_L$  and  $x_{q\Sigma} = x_{qi} + x_T + x_L$ .  $\omega_0$  is the synchronous speed of the  $i$ th generator. The units of  $\delta_i$ ,  $\omega_i$ , and  $T'_{d0i}$  are rad, rad/s, and s, respectively. The other parameters are per-unit values.

The mathematical model by Eq. (1) can be rewritten in the form of an affine nonlinear system as follows:

$$\begin{cases} \dot{x}_i(t) = f_i(x_i(t)) + g_i(t)u_i(t) \\ y_i(t) = h_i(x_i(t)) \end{cases} \tag{3}$$

where  $x_i = [\delta_i, \omega_i, E'_{qi}]^T$  is the state vector of the system,  $u_i(t) = U_{fi}$  is the  $i$ th control vector,  $y_i(t) = h_i(x_i(t)) = U_{ii}$  is the  $i$ th output vector,  $g_i(t) = \left[ 0, 0, \frac{1}{T'_{d0i}} \right]^T$  is the known functional matrix, and

$$f_i(x_i(t)) = \begin{bmatrix} \omega_i - \omega_0 \\ \frac{\omega_0}{H_i}(P_{mi} - P_{ei}) - \frac{D_i}{H_i}(\omega_i - \omega_0) \\ -\frac{E'_{qi}}{T'_{d0i}} - \frac{1}{T'_{d0i}} \frac{(x_{di} - x'_{di})}{x'_{d\Sigma}} U_s \cos \delta_i \end{bmatrix} \text{ is the known nonlinear function vector.}$$

### 3.2 Generator excitation control system based on ILC and MFAGPC

The generator excitation control system is constructed with the terminal voltage regulation as the master and independent control (Fig. 1). The output of the ILC controller drives the set point of the MFAC controller. ILC is employed to complete the tracking of terminal voltage while MFAC is employed to stabilize the system and overcome the effects of the internal and external disturbances on the system. ILC and MFAC complement each other's advantages.

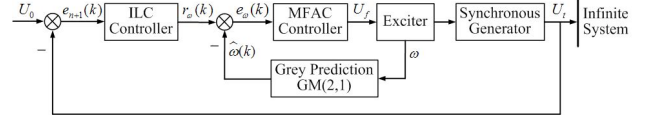


Fig. 1. Structure of excitation control system

As a given value ( $U_0$ ), the bus voltage is compared with the terminal voltage ( $U_i$ ) to obtain the error  $e(k)$ . After the closed-loop ILC operation, a new output is obtained, which is the given value  $r_{\omega}(k)$  of the MFAC controller. The deviation between  $r_{\omega}(k)$  and the predicted value  $\hat{\omega}(k)$  of the GM(2,1) model is controlled by MFAC to determine the excitation voltage.

### 3.3 ILC with initial state learning design of terminal voltage

After comparison between  $U_0$  and  $U_i$ , the constant-value control is realized by the primary controller. The discrete closed-loop PI-type ILC algorithm with initial state learning is used as the control law, as shown in Fig. 2. The closed-loop control not only accelerates learning convergence but also enhances the robustness of the learning control. At the same time, the initial state is learned, allowing an initial state error to relax the requirement on initial state positioning. The closed-loop PI-type ILC and initial state learning law are expressed as follows:

$$u_{n+1}(k) = u_n(k) + P_c e_{n+1}(k) + I_c \sum_{j=1}^{k-1} e_{n+1}(j) \tag{4}$$

$$x_{n+1}(0) = x_n(0) + L e_n(0) \tag{5}$$

where  $n$  is the number of iterations.  $k(k = 0, 1, L, N)$  is the sampling time of the discrete system.  $P_c$  and  $I_c$  are bounded learning gain matrixes of proportion and integral terms.  $L$  is the bounded gain of initial state learning law.  $e_{n+1}(k) = y_d(k) - y_{n+1}(k)$  is the tracking error at  $k$  in the  $n+1$  run.  $y_d(k)$  is the desired output.  $y_{n+1}(k)$  is the actual output of the  $n+1$  iteration. Similarly,  $u_d(k)$  and  $x_d(k)$  are the desired control variable and state vector.  $u_{n+1}(k)$  and  $x_{n+1}(k)$  are the actual control variable and state vector of the  $n+1$  iteration.

For the nonlinear system in Eq. (3), we assume that the functions  $f(x)$  and  $g(k)$  are continuous in the time interval  $k \in [0, T]$ , and  $h(x)$  has partial derivatives. They satisfy the following conditions:

(1)  $f(x)$  meets the Lipschitz condition. In other words, a constant  $l_f > 0$  exists. For  $x_1, x_2 \in R^n$ , we have  $\|f(x_1) - f(x_2)\| \leq l_f (\|x_1 - x_2\|)$ .

(2)  $h(x)$  has the derivative  $h_x(x)$  in relation to  $x$ .  $h_i(x)$  meets the global consistent Lipschitz condition and  $h_x(x)$  is bounded.

(3) The desired trajectory  $y_d(k)$  is expected to be continuous on  $[0, T]$ .

(4) An ideal control variable  $u_d(k)$  exists to make the state vector and output as the expected values  $x_d(k)$  and  $y_d(k)$ .

(5) The initial state at each iteration is different and the initial state of the  $n$  iteration is  $x_n(0)$ .

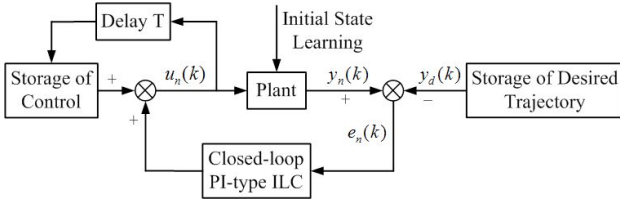


Fig. 2. Structure of ILC system

For simplicity, the following notations are used:

$$a_0 = \left( l_f g P_c + l_f g I_c \frac{1 - e^{-\lambda T}}{\lambda} \right) \frac{1 - e^{-(l_f - \lambda)T}}{\lambda - l_f}$$

$$\delta x_n = x_{n+1} - x_n$$

$$\xi_n = x_n + \gamma \delta x_n, 0 \leq \gamma \leq 1$$

$$c_x = \sup_{k \in [0, T]} \|h_x(\xi_n)\|$$

$$\rho = \frac{1}{1 - c_x a_0}$$

$$M_1 = \frac{c_x L}{1 - c_x a_0}$$

**Theorem:** If system (3) satisfies the above hypotheses and the following equation  $\|e_{n+1}\|_\lambda \leq \rho \|e_n\|_\lambda + M_1 \|e_n(0)\|_\lambda$  on  $[0, T]$  and  $0 \leq \rho < 1$  under two learning laws, when the selected  $\lambda$  is adequately large to make  $1 - c_x a_0 > 0$  and  $0 \leq M_1 < 1$ , then  $\lim_{n \rightarrow \infty} \|e_n\|_\lambda = 0$  when  $n \rightarrow \infty$ .  $y_n(k)$  converges at  $y_d(k)$  on  $[0, T]$ .

### 3.4 MFAGPC design of rotor speed

In the excitation control system, the system stability should be considered along with the high-accuracy regulation of terminal voltage. The MFAGPC of the rotor speed [18, 25] is designed to improve the system stability.

Grey prediction control uses the system behavior data as the sampling information and constructs the grey prediction model according to the metabolism principle to predict the system behavior data in the future. Then, the predicted and given values are compared to realize the advanced control. As the GM(2,1) model can reflect monotonous, non-monotonous, and oscillating dynamic processes, the GM(2,1)

model is applied to predict the sampling sequence.  $r_\omega(k)$  is the given value of MFAC,  $\omega$  is the sampling value, and  $\hat{\omega}$  is the predicted value of  $\omega$ .

#### 3.4.1 Construction steps of GM(2,1) model

The original sequence is obtained through equal interval sampling of  $\omega$  as follows:

$$\omega^{(0)} = \{\omega^{(0)}(1), \omega^{(0)}(2), \dots, \omega^{(0)}(N)\} \quad (7)$$

##### (1) Preprocessing of original sequence

Based on an accumulation of  $\omega^{(0)}$ , the accumulative sequence is

$$\omega^{(1)} = \{\omega^{(1)}(1), \omega^{(1)}(2), \dots, \omega^{(1)}(N)\} \quad (8)$$

$$\text{where } \omega^{(1)}(k) = \sum_{j=1}^k \omega^{(0)}(j), k = 1, 2, \dots, N.$$

According to the once accumulative reduction of  $\omega^{(0)}$ , the following accumulative reduction sequence is obtained:

$$\alpha^{(1)} \omega^{(0)} = \{\alpha^{(1)} \omega^{(0)}(2), \alpha^{(1)} \omega^{(0)}(3), \dots, \alpha^{(1)} \omega^{(0)}(N)\} \quad (9)$$

where  $\alpha^{(1)} \omega^{(0)}(k) = \omega^{(0)}(k) - \omega^{(0)}(k-1), k = 2, 3, \dots, N$ .

##### (2) Establishment of GM(2,1) model

The near-mean sequence is constructed by  $\omega^{(1)}$  as follows:

$$Z^{(1)} = \{Z^{(1)}(2), Z^{(1)}(3), \dots, Z^{(1)}(N)\} \quad (10)$$

where  $Z^{(1)}(k) = 0.5(\omega^{(1)}(k) + \omega^{(1)}(k-1)), k = 2, 3, \dots, N$ .

The albinism differential equation of the GM(2,1) model is

$$\frac{d^2 \omega^{(1)}}{dt^2} + a_1 \frac{d\omega^{(1)}}{dt} + a_2 \omega^{(1)} = b \quad (11)$$

After discretization, the following is obtained:

$$\alpha^{(1)} \omega^{(0)}(k) + a_1 \omega^{(1)}(k) + a_2 Z^{(1)}(k) = b, k = 2, 3, \dots, N \quad (12)$$

##### (3) Estimation of coefficients $a_1$ , $a_2$ , and $b$

The above three coefficients are identified by the least squares method.

$$\text{Let } B = \begin{bmatrix} -\omega^{(0)}(2) & -Z^{(1)}(2) & 1 \\ -\omega^{(0)}(3) & -Z^{(1)}(3) & 1 \\ \dots & \dots & \dots \\ -\omega^{(0)}(N) & -Z^{(1)}(N) & 1 \end{bmatrix} \quad \text{and}$$

$$Y = \begin{bmatrix} \alpha^{(1)} \omega^{(0)}(2) \\ \alpha^{(1)} \omega^{(0)}(3) \\ \dots \\ \alpha^{(1)} \omega^{(0)}(N) \end{bmatrix}, \text{ then } \begin{bmatrix} \hat{a}_1 \\ \hat{a}_2 \\ \hat{b} \end{bmatrix} = (B^T B)^{-1} B^T Y.$$

##### (4) Quadratic estimation of parameters

Estimated values  $\hat{a}_1$ ,  $\hat{a}_2$ , and  $\hat{b}$  of three parameters are brought into the albinism differential equation.  $\hat{\omega}^{(1)}(k)$  is solved according to the characteristic root.

(5) Construction of prediction formula

The predicted value of  $\omega^{(0)}$  is

$$\begin{cases} \hat{\omega}^{(0)}(1) = \hat{\omega}^{(1)}(1) \\ \hat{\omega}^{(0)}(k+1) = \hat{\omega}^{(1)}(k+1) - \hat{\omega}^{(1)}(k), k=1,2,\dots,N-1 \end{cases} \quad (13)$$

A new GM(2,1) model is obtained based on the preceding steps, and the new sequence is predicted and controlled.

### 3.4.2 MFAC method

MFAC performs an online estimation of the pseudo-partial-derivative (PPD) by I/O data and replaces the general nonlinear system by the dynamic linear mathematical model in incremental form, thereby stabilizing the disturbance of the system effectively.

As shown in Fig. 1,  $\omega(k)$  and  $u(k)$  are the output and input of the system at  $k$ . Let

$$\begin{cases} \Delta\omega(k+1) = \omega(k+1) - \omega(k) \\ \Delta u(k) = u(k) - u(k-1) \end{cases}, \quad (14)$$

then the compact-form linear model of the system is

$$\Delta\omega(k+1) = \Phi^T(k)\Delta u(k) \quad (15)$$

where  $\Phi^T(k)$  is the PPD of the system and  $\|\Phi^T(k)\| \leq a$ , where  $a$  is the positive real number.  $\omega(k)$  is the rotor speed at  $k$ .  $u(k)$  is the output of the MFAC controller at  $k$ .

The estimation criterion function of PPD is defined as

$$J(\Phi(k)) = \left| \omega(k) - \omega(k-1) - \Phi^T(k)\Delta u(k-1) \right|^2 + \mu \left\| \Phi(k) - \hat{\Phi}(k-1) \right\|^2 \quad (16)$$

where  $\hat{\Phi}(k)$  is the online estimation value of system PPD and  $\mu > 0$  is the penalty factor.

The extremum of Eq. (16) is calculated, and the PPD estimation algorithm of the system at  $k$  can be written as

$$\begin{aligned} \hat{\Phi}(k) &= \hat{\Phi}(k-1) + \frac{\eta\Delta u(k-1)}{\mu + \left\| \Delta u(k-1) \right\|^2} \times \\ &\left[ \Delta\omega(k) - \hat{\Phi}^T(k-1)\Delta u(k-1) \right] \end{aligned} \quad (17)$$

If  $\left\| \hat{\Phi}(k) \right\| \leq \varepsilon$  or  $\left\| \Delta u(k-1) \right\| \leq \varepsilon$ , then  $\hat{\Phi}(k) = \Phi(1)$  exists.

To prevent the algorithm from generating excessive control variables, thereby destroying the excitation system, the following control input criterion function is applied:

$$J(u(k)) = \left| r_\omega(k) - \hat{\omega}(k) \right|^2 + \lambda \left| u(k) - u(k-1) \right|^2 \quad (18)$$

where  $\eta \in (0,1]$  is the step length factor and  $\lambda > 0$  is the weighting factor.  $\varepsilon$  is the infinitely small positive real number.

The linear model is brought into the criterion function to calculate the extremum of Eq. (18). Based on the result, the following control law can be written:

$$u(k) = u(k-1) + \frac{\rho\hat{\Phi}(k)}{\lambda + \left\| \hat{\Phi}(k) \right\|^2} (r_\omega(k) - \hat{\omega}(k)) \quad (19)$$

where  $\rho \in (0,1]$  is the step length factor.

The control variable obtained from Eq. (19) is the excitation voltage  $U_f$ .

## 4. Result Analysis and Discussion

### 4.1 Simulation study

In this study, the 2-zone 4-machine system in Fig. 3 was analyzed by the proposed excitation control method based on ILC and MFAGPC. The proposed control method was compared with the open-loop ILC based on the terminal voltage bias and the conventional PID+PSS excitation control method. System parameters were introduced in reference [26]. The input mechanical power keeps constant during simulation and the initial working point of the system was chosen randomly:  $\delta_{10}=55^\circ$ ,  $P_{m10}=0.65$ ,  $U_{i10}=1.02$ ;  $\delta_{20}=37^\circ$ ,  $P_{m20}=0.85$ ,  $U_{i20}=1$ ;  $\delta_{30}=5^\circ$ ,  $P_{m30}=0.7$ ,  $U_{i30}=1.01$ ;  $\delta_{40}=25.0^\circ$ ,  $P_{m40}=0.8$ ,  $U_{i40}=1$ ;  $\omega_0=314.16$ ;  $U_s=1$ . For the  $i$ th generator,  $U_{f0}=1$  and the excitation voltage limit is  $|U_{fi}| \leq 4$ , where  $i=1,2,3,4$ . The subscript 0 denotes the initial value.

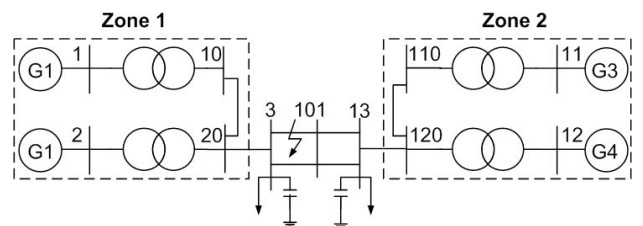


Fig. 3. 2-zone 4-machine power system

Controller parameters are set before the simulation.

(1) In ILC,  $P_c = 13$ ,  $I_c = 6.7$ , and  $L = 7$ .

(2) MFAGPC: In the GM(2,1) model, the modeling dimension  $N=5$ , initial input value  $u(1)=u(2)=0$ , and initial output value  $\omega(1)=\omega(2)=\omega(3)=0$ . In MFAC, penalty factor  $\mu = 0.65$ , step length factor  $\eta = 0.32$  and  $\rho = 0.75$ , and weighting factor  $\lambda = 1.5$ .

The system being tested runs from the equilibrium point. In the simulation, the preset fault was introduced as follows. The three-phase-to-ground short-circuit fault close to bus 3 of line 3-101 occurred at  $t=1$  s. The fault line was cleared and line 13-101 was tripped out at  $t=1.15$  s. The

corresponding curves were studied based on the generator G1.

Response curves of the terminal voltage, active power, power angle, and rotor speed of the synchronous generator under three control methods are shown in Fig. 4. The dotted line represents the open-loop ILC algorithm, the dashed line represents the conventional PID+PSS excitation control method, and the solid line represents the proposed method based on ILC and MFAGPC. Fig. 4(a) demonstrates that all the three control methods can make the terminal voltage return to the steady state after a certain period. Under the open-looped ILC, the system takes 1.7 s to return to the steady state with approximately 20% overshooting. Under PID+PSS, the settling time is approximately 1.8 s and the overshoot is around 10%. Under the collaborative effect of ILC and MFAGPC, the settling time and overshoot are approximately 0.6 s and 8%. The proposed excitation control method achieves flatter waveform, shorter time, and higher regulation accuracy of the terminal voltage. Fig. 4(b) shows that compared with the other two control methods, the proposed method based on ILC and MFAGPC can stabilize mechanical oscillation at transient state more quickly and achieves better damping feature and active power tracking performance. In addition, Figs. 4(c) and 4(d) reveal that under the open-loop ILC, the transient process of the power angle and rotor speed takes 2.3 s and 1.8 s, respectively. Under the conventional PID+PSS, the transient process of the power angle and rotor speed takes 2 s and 1.4 s, respectively. Under the ILC and MFAGPC effect, the transient process of the power angle and rotor speed takes 1 s and 1.2 s, respectively. The power angle curves reach relative stability after 4 oscillations under the open-loop ILC and after 3 oscillations under the PID+PSS, but only after 1 oscillation under the ILC and MFAGPC effect. These results indicate that the proposed excitation control method has strong damping ability and can inhibit the influence of disturbance on the system. The response curve of the relative power angle  $\delta_{31}$  between generators 3 and 1 is shown in Fig. 5. After the first oscillation of the power angle, the proposed method can recover  $\delta_{31}$  to the initial equilibrium state more quickly and shows a smaller amplitude of swing than the two other methods. The proposed method effectively maintains the transient stability of the system. As the terminal voltage is only regulated by the open-loop ILC without considering the influence on system stability, the corresponding waveforms of the terminal voltage, active power, power angle, and rotor speed fluctuate acutely with damping capacity as the worst performer. The PID+PSS method considers both the terminal voltage and system stability; thus, it is superior to the open-looped ILC in stability. However, the PID+PSS method is designed based on a precise linear model of the system. Therefore, this method involves a single parameter setting and poor adaptability and is inferior to the proposed method in terms of the voltage regulation and system stability.

#### 4.2 Experimental study

To verify the feasibility of the proposed excitation control method, a unit composed of a 3 kW DC motor and a 3 kW synchronous generator is used on the excitation regulation device that applies TMS320F28335 chip as the internal control core to simulate the single-machine infinite bus power system.

#### 4.2.1 Experimental platform

The experimental platform mainly consists of an excitation regulation control table, a DC motor, and a three-phase AC synchronous generator (Fig. 6). The DC motor is used as the prime mover.

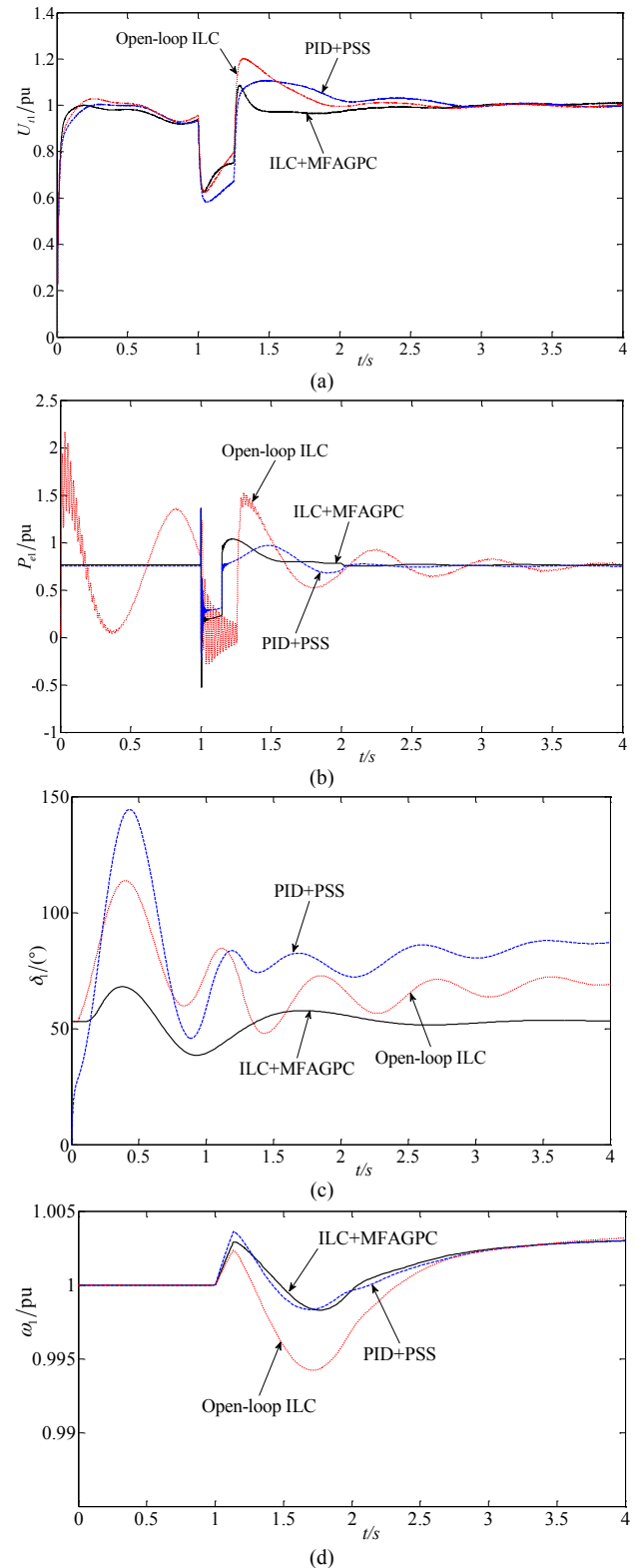


Fig. 4. Dynamic curve of generator.(a) Curves of terminal voltage. (b) Curves of active power. (c) Curves of power angle. (d) Curves of rotor speed

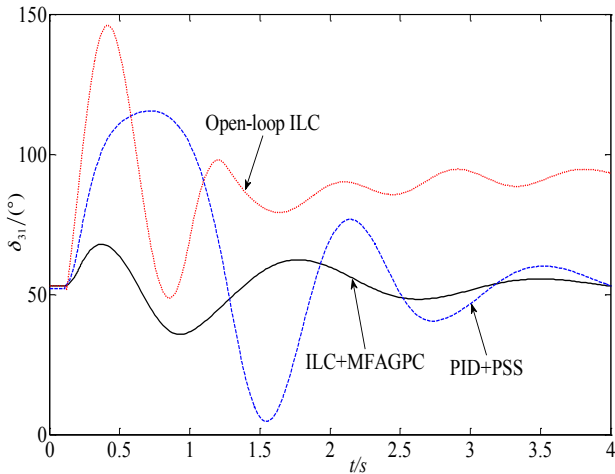


Fig. 5. Curves of relative power angle  $\delta_{31}$



Fig. 6. Experimental platform

#### 4.2.2 System parameters

The structure of the single-machine infinite-system is shown in reference [27].

**Line parameters.** Double-circuit lines are adopted between the generator and bus. Each line is  $11.5 \Omega$  and the corresponding per-unit value is 0.55,  $x_L = 0.47$ .

**Transformer parameter.** The no-load voltage ratio of the transformer is 400/800.

The prime mover used three pairs of extremely brushless DC motor. The corresponding rated power is 3 kW and the rated speed is 1500 r/min.

**Generator parameters.** Rated power = 3 kW, rated voltage = 400 V, rated current = 5.4 A, rated excitation voltage = 70 V, and rated excitation current = 3 A.

#### 4.2.3 Analysis of results

The prime mover is started first and the excitation current is regulated to make it work under the rated state. Then, a three-phase-to-ground short-circuit fault occurs at a point on the high-voltage side close to the transformer, which lasts for 0.2 s. Subsequently, the protective action is implemented and the fault line is cleared after 0.2 s. The comparison of the results between the proposed control method and conventional PID+PSS is shown in Figs.7-10.

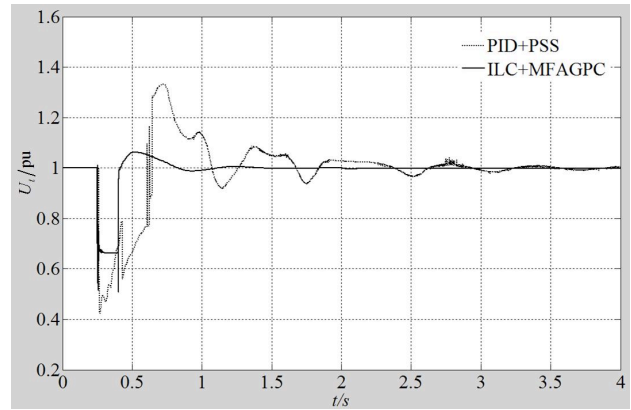


Fig. 7. Curves of terminal voltage

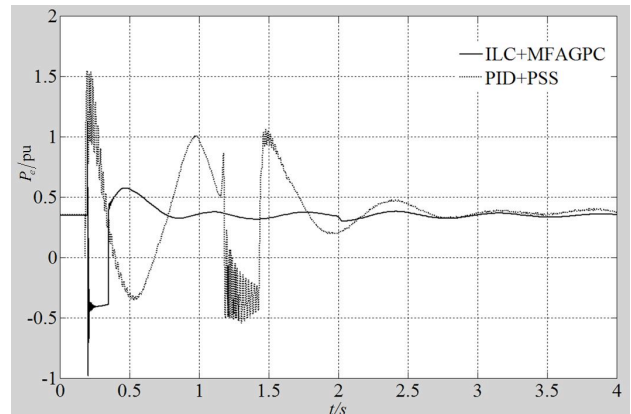


Fig. 8. Curves of active power

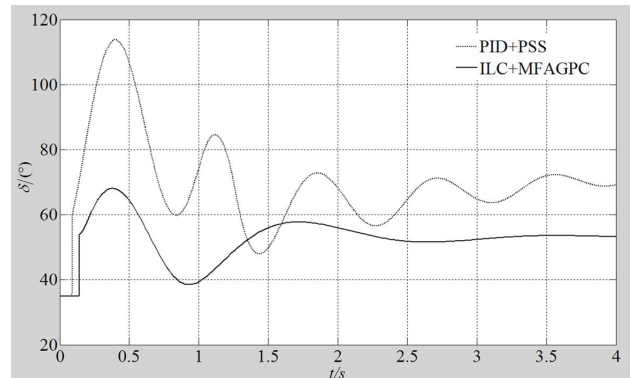


Fig. 9. Curves of power angle

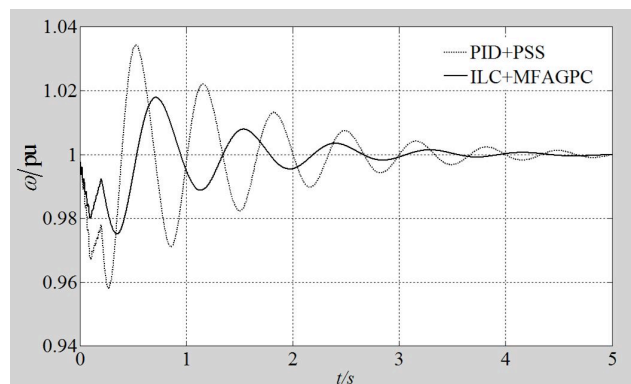


Fig. 10. Curves of rotor speed

The response curves of the terminal voltage and active power of the generator are shown in Figs. 7 and 8. Under the collaborative effect of ILC and MFAGPC, the waveform of the terminal voltage is flat. The corresponding overshoot and settling time are 7% and 0.7 s, respectively. Under

PID+PSS, the overshoot and settling time are 32% and 2.6 s, respectively. Therefore, the proposed control method can help the system achieve the desired voltage more quickly with a higher regulation accuracy of the terminal voltage. In addition, the active power fluctuates significantly at the fault occurrence under PID+PSS and settles down after 2.7 s. However, the effect of ILC and MFAGPC can prevent oscillation quickly. Overall, the control effect of the proposed method is superior to that of PID+PSS. The response curves of the power angle and rotor speed are shown in Figs. 9 and 10. After the fault, the power angle can return to rest after 3.5 s and 4 oscillations, and the rotor speed settles to a steady state after 4.3 s and 6 oscillations under PID+PSS. However, under the effect of ILC and MFAGPC, the power angle can reach stability only after 2 s and 1 oscillation, the rotor speed can reach stability after 2.5 s and 3 oscillations. Compared with PID+PSS, the proposed method based on ILC and MFAGPC has stronger damping capacity, so that the system can reach transient stability quickly.

## 5. Conclusion

To enhance the system robustness against internal and external disturbances during high-accuracy regulation of terminal voltage, the closed-loop ILC and MFAGPC were applied in the synchronous generator excitation control system based on the third-order dynamic model of the power system. Simulation and experimentation were conducted. The following conclusions could be drawn:

(1) When the control system structure is designed reasonably, ILC and MFAGPC can complement each other such that the system can obtain high-accuracy voltage regulation to ensure adequate damping capacity.

(2) The closed-loop PI-type ILC algorithm not only shortens the time for the system to reach a steady state but

also allows high-accuracy tracking of the desired voltage. Initial state also learns to adapt to the deviation of the initial working point by changes in the system parameters.

(3) Grey prediction is introduced in the MFAC method, which can enable advanced prediction of rotor speed to compensate the influences of uncertainty on the system, thereby showing robustness.

(4) Only limited parameters are considered in ILC and MFAGPC, and few coupling effects occur among these parameters.

In this study, two major excitation tasks, namely, meeting the regulation characteristics of terminal voltage and improving the system stability, are considered comprehensively. The proposed control method based on ILC and MFAGPC mirrors the actual situations of the generator excitation control system and requirements of the power system. This study provides a reference for further research on the performance of excitation systems. The experiment conducted focused only on the single-machine infinite-bus power system in a laboratory. Therefore, future studies can consider multi-machine system problems. Furthermore, the speed regulation can be introduced to change the mechanical power of the prime mover in future studies.

## Acknowledgments

This work was supported by the Key Scientific and Technological Project of Henan Province (Grant No. 182102210033) and the Key Scientific Funding Projects for Institutions of Higher Education of Henan Province (Grant No. 19B460001).

This is an Open Access article distributed under the terms of the Creative Commons Attribution Licence



## References

- Liu, Q., "Power System Stability and Generator Excitation Control". Beijing: China Power Press, China, 2007, pp.26-29.
- Kumar, A., "Power system stabilizers design for multimachine power systems using local measurements". *IEEE Transactions on Power Systems*, 31(3), 2016, pp.2163-2171.
- Isidori, A., "Nonlinear control systems". *Lecture Notes in Control & Information Sciences*, 242(65), 2003, pp.408.
- Lu, Q., Mei, S. W., Sun, Y. Z., "Nonlinear Control of Power System". Beijing: Tsinghua University Press, China, 2008, pp.257-266.
- Zhou, H. Q., Ju, P., Xue, Y. S., Li, H. Y., "Transient stability analysis of stochastic power system based on quasi-Hamiltonian system theory". *Automation of Electric Power Systems*, 40(19), 2016, pp.9-14.
- Han, Y., "Nonlinear variable structure control technique for power system excitation controllers". *Tsinghua Science & Technology*, 1(3), 2012, pp.290-294.
- Yang, J. H., Chen, K. Y., Wang, Q. J., Chen, S. Z., "Variable structure control of voltage source converter-high voltage direct current system based on backstepping". *Control Theory & Applications*, 31(11), 2014, pp.1548-1554.
- Peng, Y. J., Han, F. M., Chen, J. H., Deng, F. Q., "Synchronous generator excitation controller for random disturbance rejection". *Control Theory & Applications*, 35(4), 2018, pp.438-446.
- Mahmud, M. A., Hossain, M. J., Pota, H. R., "Transient stability enhancement of multimachine power systems using nonlinear observer-based excitation controller". *International Journal of Electrical Power & Energy Systems*, 58(1), 2014, pp.57-63.
- Su, B. L., Xin, Y. H., "Multi machine electric power control system based on the high order of excitation sliding mode". *Control Engineering of China*, 25(5), 2018, pp.760-764.
- Zhao, H., Wang, Y. F., Wang, H. J., Yue, Y. J., "Study of waste heat power generation units excitation control based on sliding mode variable structure control". *Power System Protection and Control*, 43(6), 2015, pp.8-13.
- Alden, M. J., Wang, X. "Robust control of time delayed power systems". *Systems Science & Control Engineering*, 3(1), 2015, pp.253-261.
- Masrob, M. A., Rahman, M. A., George, G. H., "Design of a neural network based power system stabilizer in reduced order power system". In: *2017 IEEE 30th Canadian Conference on Electrical and Computer Engineering*, Windsor, CAN: IEEE, 2017, pp.1-6.
- Zhao, H., Lan, X., Xue, N., Wang, B., "Excitation prediction control of multi-machine power systems using balanced reduced model". *Iet Generation Transmission & Distribution*, 8(6), 2014, pp.1075-1081.
- Ghasemi, A., Shayeghi, H., Alkhatib, H., "Robust design of multimachine power system stabilizer using fuzzy gravitational search algorithm". *International Journal of Electrical Power & Energy Systems*, 51(1), 2013, pp.190-200.
- Zhao, Y., Lu, C., Han, Y., Men, K., "Wide area power system stabilizer design based on improved model free adaptive control". *Journal of Tsinghua University*, 53(11), 2013, pp.1645-1652.
- Guo, G., Liu, J. M., Lu, W. J., Xiang, Z., "Nonlinear excitation control based on deviation separation for synchronous generator". *Proceedings of the CSU-EPSA*, 26(3), 2014, pp.31-34.

18. Zhang, W., Shi, W., Wang, G., Sun, B., "An improved model-free adaptive control of marine generator excitation system". *International Journal of Robotics & Automation*, 32(6), 2017, pp.616-624.
19. Wang, R. J., Zhan, Y. J., Zhou, H. F., Cui, B. W., "PID controlled AVR system based on differential evolution mechanism optimization". *Power System Protection and Control*, 43(24), 2015, pp.108-114.
20. Lin, T., Xu, Q. G., Xuan, Q. Q., Wu, M. X., "Study on optimal control of stability of synchronous generator excitation system". *Computer Simulation*, 34(6), 2017, pp.222-226.
21. Chang, X. R., Zhang, H. S., Cui, Z. J., "Excitation control based on differential geometry and extended state observer". *Proceedings of the CSU-EPSA*, 27(8), 2015, pp.87-91.
22. Ruan, Y., Yuan, R. X., Wan, L., Zhao, H. S., "Nonlinear robust voltage control for synchronous generators". *Transactions of China Electrotechnical Society*, 27(9), 2012, pp.9-16.
23. Yang, F., Ruan, Y., Yuan, R. X., "Nonlinear robust excitation control based on output feedback for synchronous generator". *Electric Power Automation Equipment*, 32(10), 2012, pp.65-71.
24. Yan, Q. Z., Sun, M. X., Li, H., "Iterative learning control for nonlinear uncertain systems with arbitrary initial state". *Acta Automatica Sinica*, 42(4), 2016, pp.545-555.
25. Hou, Z. S., "Highlight and perspective on model free adaptive control". *Systems Science and Mathematical Sciences*, 34(10), 2014, pp.1182-1191.
26. Kundur, P., "*Power System Stability and Control*". New York: McGraw-Hill, Inc. USA, 2001, pp.34-37.
27. Ge, B. J., Yin, J. W., Tao, D. J., Niu, Z. L., "Modeling of field-circuit-network coupled time-stepping finite element for one machine infinite bus system based on excitation and speed control". *Transactions of China Electrotechnical Society*, 32(3), 2017, pp.139-148.